Quaternary Research 80 (2013) 158–166

Contents lists available at ScienceDirect

Quaternary Research

journal homepage: www.elsevier.com/locate/yqres

A 352-year record of summer temperature reconstruction in the western Tianshan Mountains, China, as deduced from tree-ring density

Shulong Yu *, Yujiang Yuan, Wenshou Wei, Feng Chen, Tongwen Zhang, Huaming Shang, Ruibo Zhang, Li Qing

Institute of Desert Meteorology, China Meteorological Administration, 46 Jianguo Road, 830002 Urumqi, China
Key Laboratory of Tree-ring Ecology of Uyghur Autonomous Region, 46 Jianguo Road, 830002 Urumqi, China
Key Laboratory of Tree-ring Physical and Chemical Research of China Meteorological Administration, 46 Jianguo Road, 830002 Urumqi, China

ARTICLE INFO

Article history:
Received 27 November 2012
Available online 14 July 2013

Keywords:
Picea schrenkiana
Mean latewood density
Temperature reconstruction
Western Tianshan Mountains

ABSTRACT

Three robust tree-ring density chronologies were developed for the western Tianshan Mountains of northwestern China. The chronologies were significantly correlated and form a regional chronology (GLD). The GLD had significant and positive correlations with temperature of warm seasons. Based on this relationship, the mean minimum temperatures of May to August were reconstructed using the GLD chronology for the period AD 1657 to 2008. The temperature reconstruction exhibited temperature patterns on interannual to centennial timescales, and showed that the end of the 20th century is the warmest period in the past 352 years. The reconstructed temperature variation has a teleconnection with large-scale atmospheric–oceanic variability and captures long- and broad-scale regional climatic variations.

Introduction

Tree rings have been used as a high-resolution proxy for climate change. Tree-ring series, especially maximum latewood density from cold-moist sites have great potential for the reconstruction of summer temperatures on regional to hemispheric scales, reflecting inter-annual to multi-centennial scale variability (e.g., Schweingruber and Briffa, 1996; Briffa et al., 2001; Frank and Esper, 2005; Büntgen et al., 2006, 2008).

Earlier studies (Yuan and Li, 1999; Yuan et al., 2001; Yuan et al., 2003; Chen et al., 2009, 2010) have indicated the dendroclimatic utility of tree-ring width and density in the Tianshan Mountains of northwestern China. For example, Yuan and Li (1999) reconstructed the winter temperature from AD 1543 to 1995 near the Urumqi River using tree-ring width. Yuan et al. (2001) presented a 348-yr precipitation series using tree-ring width of *Picea schrenkiana* in the Urumqi River Basin. Esper et al. (2001) and Esper (2003) identified the climatic extreme years since AD 1427 and a 1300-yr climatic history for western Central Asia inferred from tree-rings, a prolonged centennial trend towards better growing conditions had been observed over the last 300 yr. A temperature reconstruction of 153 yr was established with maximum density of *P. schrenkiana* in Yili by Chen et al. (2009), and indicated a cold span in spring and summer from the beginning of the 1950s to the beginning of the 1970s. Chen et al. (2011) reconstructed summer temperatures based on the standard chronology of mean latewood density (LWD) from AD 1600 to 2002 for the Zaysan Lake area in East Kazakhstan, with pronounced cooling during the time of the Maunder (late 1600s to early 1700s), Dalton (late 1700s to early 1800s) and Damon Minima (late 1800s). These climate reconstructions make it possible to describe the recent climate history of Central Asia. However, compared to Europe and North America, the number of tree-ring investigation sites from Central Asia is small. More chronologies are needed to interpret the past climate variability over long temporal and large spatial scales.

This paper describes high-resolution, precisely dated records of warm-season annual temperature variation and tree growth for the past 3 centuries in the western Tianshan Mountains region of China. These records are based on a network of tree-ring chronologies developed for mean latewood density. The regional climate record developed for this study allows us to study climate change and investigate the effects of volcanic, solar, and other forcing factors on this regional climate. We analyze the relationships between tree-ring parameters and their climatic forcing. Based on LWD data, we reconstruct warm season (May–August) minimum temperatures over the period AD 1657–2008 of reliable internal signal strength. This new record is then compared with existing findings from nearby regions.

Material and methods

Study area

The Tianshan Mountains of Central Asia extend across Kyrgyzstan, Kazakhstan and China, with complex topography and unique natural conditions. *P. schrenkiana* forest is the most dominant and widespread

* Corresponding author.
E-mail address: yushl@idm.cn (S. Yu).

0033-5894/$ – see front matter © 2013 University of Washington. Published by Elsevier Inc. All rights reserved.
http://dx.doi.org/10.1016/j.yqres.2013.05.005

boreal forest type on the north slopes of the Tianshan Mountains, and is also one of the most important zonal vegetation types in the region, accounting for 60.8% of the timber stock and 44.9% of forest land in the Xinjiang area (Chang and Li, 1995), and dominates elevations of 1200–3000 m asl in the study area.

Tree-ring sampling and chronology development

We selected open-canopy timberline stands in Gongnaisi of the western Tianshan Mountains (Fig. 1, Table 1) in May 2009. The sites were located approximates 12–25 km apart. We obtained increment cores at breast height from a total of 88 living trees with 28–31 trees per site, with one 5 mm and one 12 mm core per tree. The 5 mm samples were cross-dated and measured using traditional dendrochronological procedures (Fritts, 1976; Cook and Kairiukstis, 1990) using a Velmex measuring system. The system precision is 0.001 mm. The 12 mm samples were cut transversely into thin sections of 1.0 ± 0.02 mm with a twin-bladed saw (DENDRO CUT 2003) and subjected to X-ray analysis on a Tree Ring Density Data Acquisition system. X-ray films were exposed using transmitted light on DENDRO XRAY2. The densitometric analysis of these X-ray films was carried out on DENDRO-2003 tree-ring workstation. The seven parameters (ring width, earlywood width, latewood width, maximum density, minimum density, mean earlywood density, mean latewood density) were measured for each annual ring on each core. Counter-checks for possible measurement and dating errors and individual ring-width series were tested against a master series derived by averaging all series on the basis of correlation computed using the program COFECHA developed by Holmes (1983). There were strong within-site common signals in the ring-width (RW) series, as indicated by an overall mean inter-series correlation of r = 0.62 (range: 0.60–0.65) in the output of COFECHA. We used mean latewood density (LWD) in this study. Each RW and LWD series was standardized (detrended) using ARSTAN program (Cook, 1985), in order to remove non-climatic, biological factors from the series. Conservative detrending methods (smoothing spline method or negative exponential curve method) were used to generate both RW and LWD chronologies in order to retain low-frequency information (Cook, 1985; Jacoby and D'Arrigo, 1989). We used the standard version of the LWD chronologies, which contains the common variations among the individual tree core series and retains low- through high-frequency common variance, presumably in response to climate (Cook, 1985).

Table 1
Information about the sampling site in Gongnaisi.

Site	Longitude (N)	Latitude (E)	Elevation (m)	Aspect	No. of trees
AKS	43°12.2′	84°47.8′	2420–2480	WS	28
BCS	43°17.4′	84°50.9′	2480–2530	NE	31
WQS	43°24.6′	84°44.6′	2560–2645	E	29

The average intercorrelation among the three RW and LWD series is 0.720 and 0.697 (Table 2). Across all three sites (88 series), the RW series inter-correlation measured 0.61. As RW variation was consistent across the sites, and the sites were located close together (<30 km), we pooled the LWD data together from all three sites to create a composite record as regional series (GLD, Fig. 2) for dendroclimatic analyses in study area.

In order to estimate the reliability of the tree-ring chronologies, the Expressed Population Signal (EPS) statistic and Rbar were calculated using ARSTAN. EPS evaluates the relationship between the sample size of a chronology and the common variance or "signal" within a chronology. Generally, a value of 0.85 or greater is considered a rough cut-off point for an acceptable level a correlation (Wigley et al., 1984). However, EPS estimates chronology confidence and should not be interpreted rigidly (ITRDB Dendrochronology Forum posting; http://listserv.arizona.edu/archives/itrdbfor/). The Rbar statistic is a measure of the average inter-correlation of all overlapping series. The running means EPS (30-yr moving window with 15-yr overlaps) is 0.91 over the entire regional LWD series common period (ranging from 0.90 to 0.97). The mean Rbar for GLD is 0.41, respectively. The GLD chronology spans AD 1618 to 2008, with a common period from 1814 to 1990, the EPS was only greater than 0.85 after AD 1657, when the sample size was 17 cores.

Meteorological data

Monthly mean temperatures and precipitation data were obtained from Xinyuan climate stations (43.45°N, 83.30°E, 929 m asl) near our sample sites from the National Meteorological Information Centre (NMIC) of China (Fig. 1). The station data includes monthly maximum, mean and minimum temperatures and precipitation from 1956 to 2008.

To provide a more regional climate signal, the gridded monthly precipitation and temperatures data near the Gongnais area, 0.5 × 0.5°square, from 1901 to 2008, were obtained from the Climatic Research Unit (CRU), East Anglia, UK, through their web site: http://

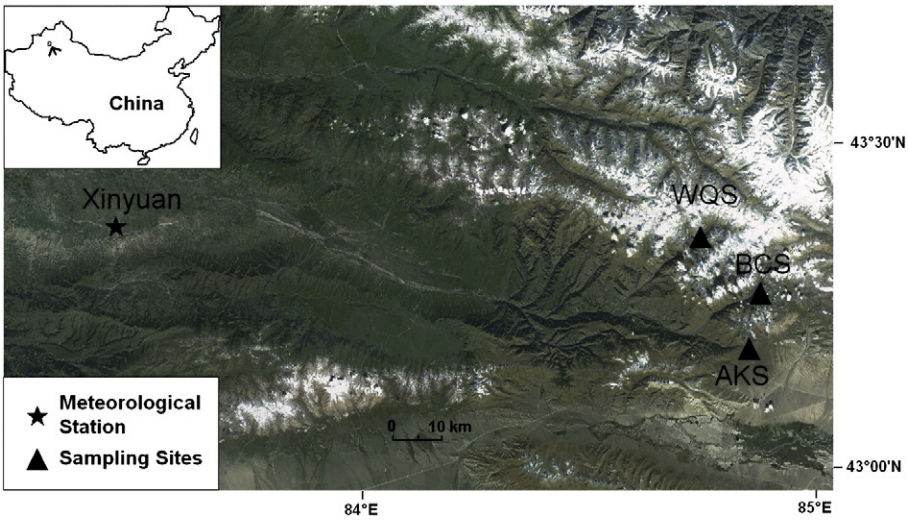

Figure 1. Location map of the tree-ring sampled sites and meteorological station.

https://doi.org/10.1016/j.yqres.2013.05.005 Published online by Cambridge University Press

Table 2
Correlation matrix for ring width (RW) and mean latewood density (LWD) from 1758 to 2008.

	RW			LWD		
	AKS	BCS	WQS	AKS	BCS	WQS
AKS	1	0.676	0.665	1	0.657	0.706
BCS		1	0.820		1	0.728
WQS			1			1

www.cru.uea.ac.uk (Mitchell and Jones, 2005), and the global sea-surface temperatures (SSTs) were taken from the Met Office Marine Data Bank (MDB), which from 1982 onwards also includes data received through the Global Telecommunications System (GTS) (Rayner et al., 2003).

Statistical analysis

The climate vs. tree latewood density relationships were investigated by using correlation analyses between tree-ring data and meteorological records for their overlap period 1956–2008. Simple correlations were calculated between the GLD standard chronology and monthly climate variables (precipitation, mean temperature as well as maximum and minimum temperatures) from October prior to growth to December of the current growth year (Fig. 3). In addition, various seasonal means of climate variables and their correlations with tree-ring data were calculated. To determine whether the relationship between tree growth and climate was stable through time, we conducted a 30-yr moving correlation analysis between the GLD and the climate data (Fig. 4). The climate variables used in the analysis include the seasonal and monthly mean, and the maximum and minimum temperatures.

Nine linear regression models between the predictors and the predictand were computed, the predictand was selected several for seasonal and monthly climate variables that had significant correlations with the GLD, including July, May–August and February–November (Table 3). As the instrumental records available were too short for independent sub-period calibration and verification tests, both the "leave-one-out cross-validation" technique (LOOCV) (Michaelsen, 1987) and bootstrapping (Guiot, 1991) were employed to check the stability and reliability of the regression models. We used 100 bootstrapped subsamples to compute the models' explained variance and adjusted explained variance. The size of each subsample was the same as that of the initial data set to avoid bias. In the LOOCV analysis, several statistics, including sign tests of both the first-differencing data (SN1) and the raw data (SN2), the reduction of error (RE), and correlation coefficients were calculated to evaluate the similarity between the observed data and the estimated data. A sign test measures the degree of association between series (or variables) by counting the number of agreements and disagreements in the two series. The series are correlated if the number of similarities is significantly larger than the number of dissimilarities. The RE statistic provides a rigorous test of association between actual and estimated data, and any positive value is considered as indicative for the predictive skill of the model (Fritts, 1976).

The multi-taper method (MTM) of spectral analysis (Mann and Lees, 1996) was applied to examine the characteristics of local climate variability in the frequency domain. The analysis was performed over the full range of our reconstruction. Our analysis used $5 \times 3\pi$ tapers and in a red noise background.

Results

Tree-growth response to climate

The GLD standard chronology was more highly correlated with temperature than with precipitation (Fig. 3). Correlation coefficients of mean and minimum temperatures revealed positive significant response from the previous October to the current December. Precipitation in the growing season and maximum temperature in the previous October and Decembers had mostly negative influences on GLD. Significant ($p < 0.001$) positive correlations were found for the mean temperature in March and May to August, the May maximum temperature and the February to November, February to August, May to September and May to August minimum temperatures. The maximum correlation appeared between the chronology and warm season (May until August) minimum temperature, it reached 0.812 ($p < 0.001$). The GLD standard chronology was not found to be

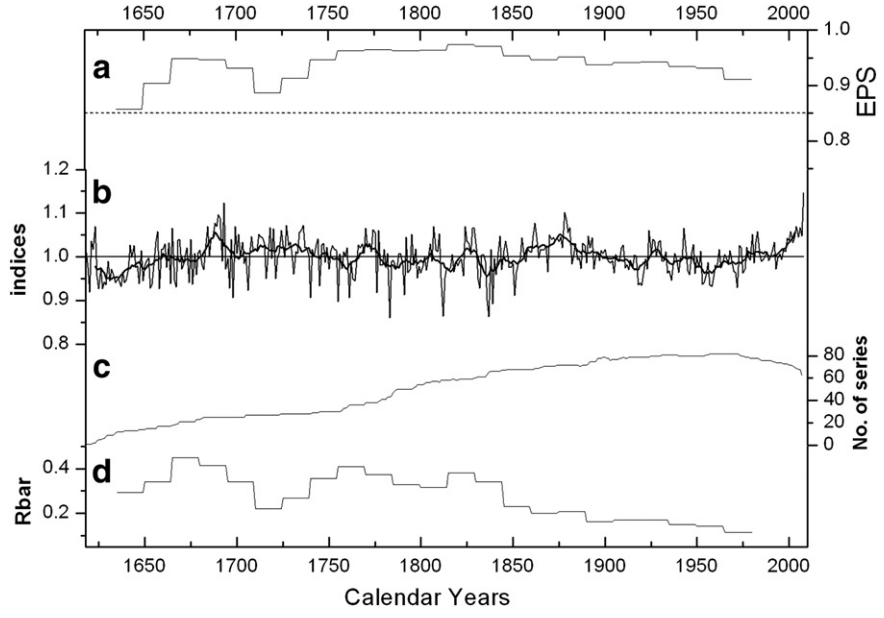

Figure 2. a. Expressed population signal (EPS) statistic (calculated over 30 yr lagged by 15 yr), the dotted line denotes the 0.85 EPS criterion for signal strength acceptance; b. the mean latewood density chronology (GLD) and its 11-yr moving average (thick solid line), AD 1618–2008; c. the sample depths through time; d. mean inter-series correlation (RBAR).

https://doi.org/10.1016/j.yqres.2013.05.005 Published online by Cambridge University Press

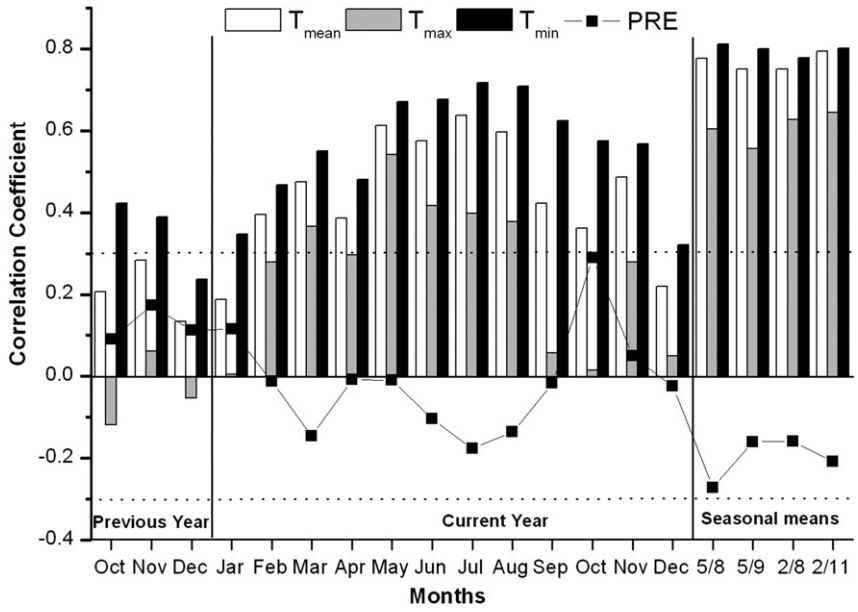

Figure 3. Climate response of the mean latewood density standard chronology (GLD) using mean temperatures (T_{mean}), maximum temperatures (T_{max}), minimum temperatures (T_{min}), and precipitation sums (PRE). Correlations were calculated from previous year October to current year December over 1956–2008 common periods. Horizontal dashed lines denote the 99% significance levels. Numbers on the x-axis refer to seasonal means of prior May–August (5/8), prior May–September (5/9), prior February–August (2/8), and prior February–November (2/11), respectively.

significantly correlated with precipitation. These results suggest that temperatures may be the primary factor limiting mean latewood density growth of *P. schrenkiana*.

Correlations between the GLD and temperatures may not be stable through time (Fig. 4). For example, there was a steep decrease from 2000 to 2003, and a steep increase after 2003 in the moving correlation with the July temperature. In contrast, the moving correlations with minimum temperature were best for May–August and February–November temperatures. There were an increased trend after 2003 and a gradual decrease in trend among 1986–1989 in the moving correlation with the three types of seasonal temperatures, while the other relationships remained relatively stable. The latewood density showed a positive association with temperature for growing periods (May–August) when latewood is formed, but there was no association with precipitation.

In closing this section, it can be concluded that the growing season (May–August) temperature is well represented by at least one of the tree-ring parameters, and thus suitable for its reconstruction.

Temperature reconstruction

Based on the results of the growth-climate analyses, we tried a number of combinations of seasonal temperature variables for our calibration test (Table 3). The transfer functions used GLD standard chronology as the independent variable. It should be noted that GLD can describe variation in the annual mean maximum and minimum temperatures (July, May–August and February–November). The maximum value of explained variance in the full-period calibration by the regression model was in the May–August minimum temperatures ($R^2 = 66.0\%$), the correlation coefficient between the temperature

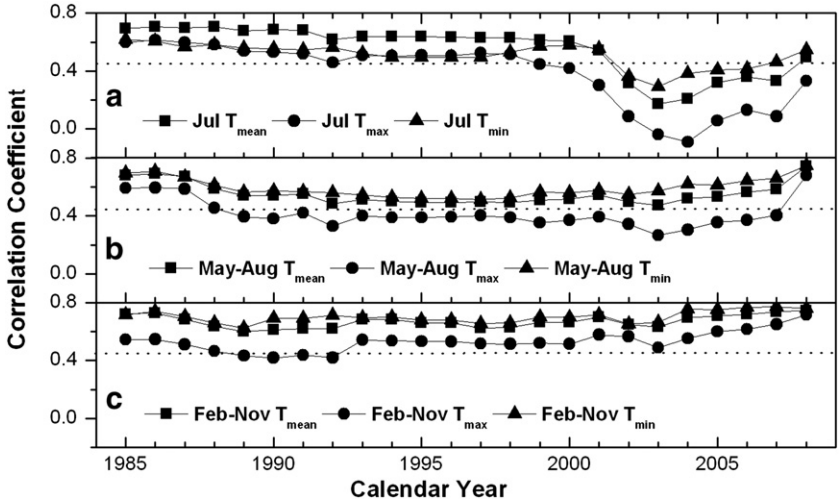

Figure 4. 30-yr moving correlations between the GLD and seasonal mean climate variables. a. July; b. May–August; c. February–November. The years are the final years of each moving interval. The dotted horizontal line denotes 99% significance levels.

https://doi.org/10.1016/j.yqres.2013.05.005 Published online by Cambridge University Press

Table 3
Calibration and cross-validation statistics of the monthly/seasonal temperature models for the reconstruction during AD 1657–2008. We used the leave-one-out cross-validation (LOOCV) method and the bootstrap analysis to test the stability and reliability of the regression models. R, correlation coefficient; R^2/R_a^2, explained variance and adjusted explained variance; SN1/SN2, the first-differencing data and the raw data sign test; RE, reduction of error. Any positive value of RE indicates that there is confidence in the reconstruction (Fritts, 1976).

Variable	Season	Calibration			LOOCV				Bootstrapped mean (minimum, maximum)	
		R	R^2	R_a^2	SN1	SN2	RE	R^2	R^2	R_a^2
T_{mean}	July	0.638**	0.408	0.396	31+/21−	34+/19−	0.366	0.368	0.412(0.132,0.631)	0.401(0.115,0.624)
T_{mean}	May–Aug	0.778**	0.605	0.597	36+/16−**	43+/10−**	0.579	0.579	0.624(0.392,0.793)	0.617(0.380,0.789)
T_{mean}	Feb–Nov	0.795**	0.632	0.625	40+/12−**	42+/11−**	0.589	0.592	0.634(0.440,0.762)	0.627(0.429,0.757)
T_{max}	July	0.400*	0.160	0.144	28+/24−	31+/22−	0.104	0.108	0.166(0.001,0.369)	0.149(0.000,0.357)
T_{max}	May–Aug	0.606**	0.367	0.355	33+/19−	35+/18−*	0.310	0.310	0.372(0.098,0.700)	0.360(0.080,0.695)
T_{max}	Feb–Nov	0.646**	0.417	0.406	37+/15−**	37+/16−**	0.381	0.382	0.428(0.180,0.622)	0.417(0.164,0.615)
T_{min}	July	0.719**	0.516	0.507	31+/21−	36+/17−*	0.474	0.476	0.514(0.277,0.629)	0.504(0.263,0.621)
T_{min}	May–Aug	0.812**	0.660	0.653	34+/18−*	41+/12−**	0.628	0.629	0.661(0.450,0.802)	0.654(0.440,0.798)
T_{min}	Feb–Nov	0.803**	0.644	0.637	38+/14−**	40+/13−**	0.587	0.592	0.654(0.498,0.768)	0.647(0.488,0.763)

T_{mean} = mean temperature, T_{max} = mean maximum temperature, T_{min} = mean minimum temperature, +/− is the signs (positive or negative) of the subtraction of consecutive years' values.
* $p < 0.05$.
** $p < 0.01$.

reconstruction and Xinyuan stations date was 0.812 ($p < 0.01$). Results of the sign test in the raw (SN2) and in first-differenced (SN1) data passed significance test ($p = 0.05$), the reduction of error (RE) was positive. The LOOCV ($R^2 = 62.9\%$) and bootstrap analysis ($R^2 = 66.1\%$) indicate that the model is of acceptable stability and reliability, and can simulate May–August minimum temperatures with good accuracy. On the basis of this model ($T_{min5-8} = -10.5 + 23.2 \times GLD$), May–August minimum temperatures in the study area has been reconstructed for the period AD 1657–2008 (Fig. 5).

In addition, other models except for the July maximum temperature are reasonably accurate, as indicated by the high value of explained variance and by the significant ($p < 0.05$) statistics in the LOOCV and bootstrap analysis (Table 3).

The characteristics of the temperature reconstruction

Fig. 5 shows the unfiltered and 8-yr low-pass filtered May–August minimum temperatures in Gongnaisi of the western Tianshan Mountains from AD 1657 to 2008. The mean of May–August minimum temperatures over the period (1657–2008) is 12.68°C. The years 1783 (9.35°C) and 2008 (15.70°C) are reconstructed as the most extreme years. The reconstruction revealed a warmer period from 1657 to 1738, followed by a lower temperatures periods from 1738 to 1854. Temperature over the past 150 yr indicates two warmer periods (1855–1899, 1977–2008) and one cooler period (1900–1976). Decadal means for the 2000s rank among the warmest decades. The warmest years are distributed throughout the 17th, 19th, and 21st centuries (1665, 1688, 1690, 1691, 1693, 1862, 1878, 1879, 2004, 2008; Table 4), and the coldest years are more widely distributed throughout the sequence (1698, 1740, 1755, 1761, 1783, 1791, 1812, 1836, 1837, 1839) and the coldest decades are divided equally between the 19th (1810s, 1830s) and 20th centuries (1910s, 1950s).

The MTM analysis was performed over the full range of our reconstruction sequence. This analysis revealed some significant low- and high-frequency cycles. The century-scale cycle (period = 170.7 yr) is most significant in our reconstruction. Two decadal broadband

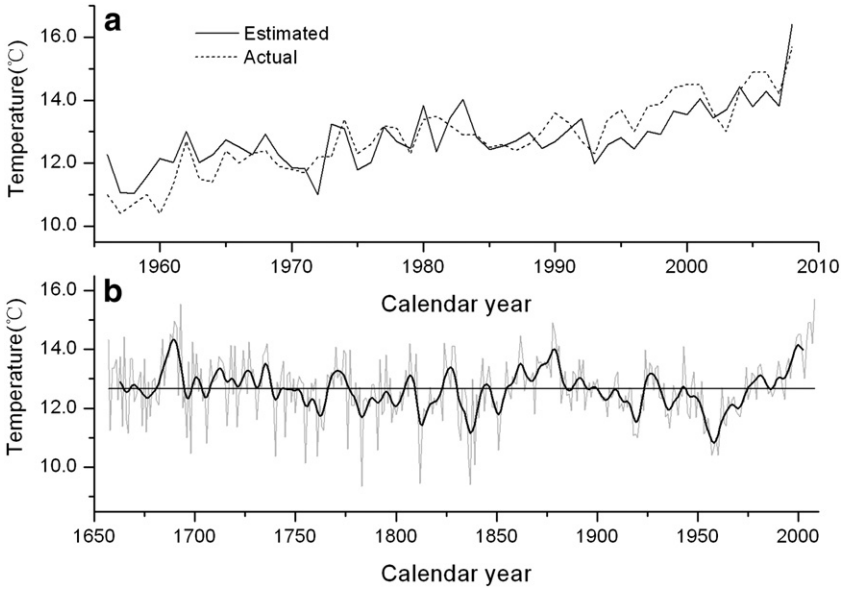

Figure 5. a. Comparison between actual and estimated mean season (May to August) minimum temperature for their common period 1956–2008; b. temperature reconstruction for the central derived from latewood density. Thin line represents annual values; the bold line was smoothed with an 8-yr low-pass filter; horizontal line was average of reconstruction from AD 1657 to 2008.

https://doi.org/10.1016/j.yqres.2013.05.005 Published online by Cambridge University Press

Table 4
Summary characteristics of the May–August minimum temperature reconstruction: anomalies are calculated with respect to the AD 1657–2008 mean.

10 Most extreme years				10 Warmest and coldest decades				Long-term means	
Year	Coldest (°C)	Year	Warmest (°C)	Decade	Coldest (°C)	Decade	Warmest (°C)	Period	Value (°C)
1783	9.35	1665	14.42	1830	10.694	1770	12.97	1657–1738	13.00
1837	9.42	2004	14.42	1950	11.75	1820	13.03	1739–1854	12.37
1812	9.44	1862	14.47	1810	11.90	1730	13.03	1855–1899	13.12
1839	10.09	1688	14.51	1910	12.13	1720	13.10	1900–1976	12.30
1755	10.14	1879	14.54	1780	12.13	1710	13.11	1977–2008	13.23
1836	10.28	1691	14.77	1760	12.27	1860	13.13		
1740	10.37	1878	14.91	1790	12.29	1690	13.16		
1761	10.37	1690	14.95	1970	12.31	1680	13.40		
1698	10.46	1693	15.53	1930	12.32	1870	13.74		
1791	10.58	2008	15.70	1750	12.36	2000	14.09		

power peaks (periods: 18.3, and 26.3 yr) were identified for temperature variability. Significant high-frequency peaks were found at 4.9, 3.6, 3.0, 2.5, 2.4, 2.3, 2.1 and 2.0 yr (Fig. 6).

Discussion

Natural forces

Tree-ring density data derived from trees sampled at high elevations displayed a strong correlation with warm-season temperature measurements over large areas of northern America and Eurasia, demonstrating the ability of this proxy to portray warm-season temperature changes on large scales and across sub-continental scales (Polge, 1970; Briffa et al., 1988; Schweingruber et al., 1988; Briffa et al., 1992; Schweingruber et al., 1993; Luckman et al., 1997; Briffa et al., 2001; Davi et al., 2002; Wilson and Luckman, 2003; Bräuning and Mantwill, 2004; Wang et al., 2009). The chronologies from *P. schrenkiana* in the western Tianshan Mountains show similar temperature sensitivity indices in the warm season (May–August). Conifer tracheids divide and enlarge most actively during the warmest period of the growing season, and warm temperatures during this period can promote earlier snowmelt and more rapid warming of soils, thereby increasing the growing season length and resulting in faster leaf, shoot, and stem growth (Körner, 1998; Peterson and Peterson, 2001). Alward et al. (1999) hypothesized that elevated night time minimum temperature would cause an increase in nocturnal respiration rates in grassland vegetation without a compensatory increase in daytime photosynthesis. A similar process applies to tree rings as night time minimum temperatures increase. High night time temperatures may inhibit growth in cell size and be conducive to the accumulation of nutrients. The processes in warm season can form a larger mean latewood density in that year. The climatic variable most strongly correlated to density growth is also summer temperature for western North America (Briffa et al., 1992), Canada (Luckman et al., 1997), Japan (Davi et al., 2002), Scandinavia and Switzerland (Schweingruber et al., 1988), eastern Tibet (Wang et al., 2009). Unlike the widely reported 'divergence problem' in northern forests (Briffa et al., 1998a; D'Arrigo et al., 2008), spruce growth of the western Tianshan Mountains did not clearly lose sensitivity to recent warming in our study area. The most recent warming trend is reflected most clearly by the latewood density data (Fig. 5).

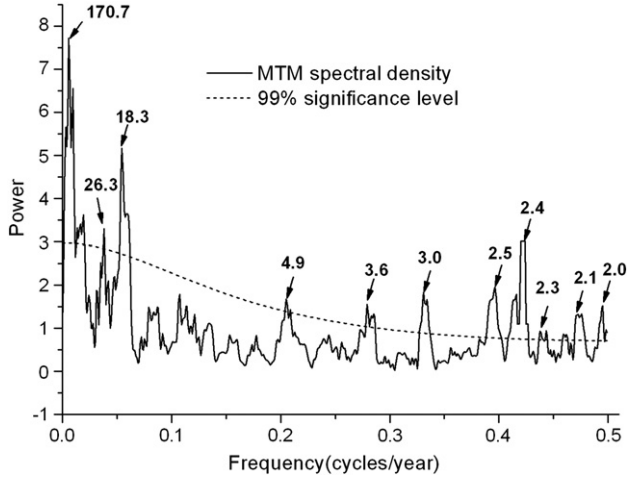

Figure 6. Multi-taper method (MTM) spectral density of the May–August minimum temperature reconstruction. Bold line indicates the null hypothesis; dashed line indicates the 99% significance levels, respectively. Numbers above peaks indicate cycle intervals (yr).

Many low tree-ring density value years were forced by volcanic eruptions in the Northern Hemisphere (Jones et al., 1995; Briffa et al., 1998b). Several studies (LaMarch and Hirschboeck, 1984; Briffa et al., 1998b; D'Arrigo and Jacoby, 1999; Gervais and MacDonald, 2001; Luckman and Wilson, 2005) found a cooling response to volcanic eruptions. Comparison of our reconstruction with volcanic eruptions reveals that there is no systematic relationship between reconstructed sequences and volcanic eruption, and is likely related to the regional character of both the Gongnaisi temperature and forcing data (Simkin and Siebert, 1994). From the temperature reconstruction in this study, 10 years were found to have low values, associated with volcanic eruptions. Examples include Tongkoko in Sulawesi (1680), Komaga-take in Japan (1695), Shikotsu in Japan (1739), Taal in Indonesia (1754), Laki in Iceland (1783), St Helens in the US (1800), Awu in Indonesia (1812), Tambora in Indonesia (1815), Okataina in New Zealand (1886) and Novarupta (Katmai) in Alaska (1912).

Peaks at ~2 to 5 yr cycles fall within the range of variability of the El Niño–Southern Oscillation (Allan et al., 1996), and the peaks at ~2 yr are also within the band of tropical biennial oscillation (TBO) variability (Meehl, 1987). Collectively, these periods suggest that the reconstructed temperature variation has a teleconnection with large-scale atmospheric–oceanic variability. Peaks at 18.3 and 26.3 yr may correspond to similar periods found in a reconstructed Pacific decadal oscillation series from the Transverse Mountains of southern California (USA) to Sierra San Pedro Martir in northern Baja California, Mexico (Biondi et al., 2001). The peak at 170.2 yr could fall within the Suess cycle of solar activity.

Regional- to large-scale comparison

To further assess the validity of our temperature reconstruction for the Gongnaisi region, we compared it with other summer temperature reconstructions from nearby (Chen et al., 2009; Chen et al., 2011). As our reconstruction was most similar to a summer (June–August) temperature reconstruction for the Zaysan Lake area (Chen et al., 2011) for the years 1657–2002, the correlation coefficient was 0.265 ($p < 0.01$), and increasing coherence after 8-yr low-pass filtering (0.296), the change trend of two series was same from 1657 to

https://doi.org/10.1016/j.yqres.2013.05.005 Published online by Cambridge University Press

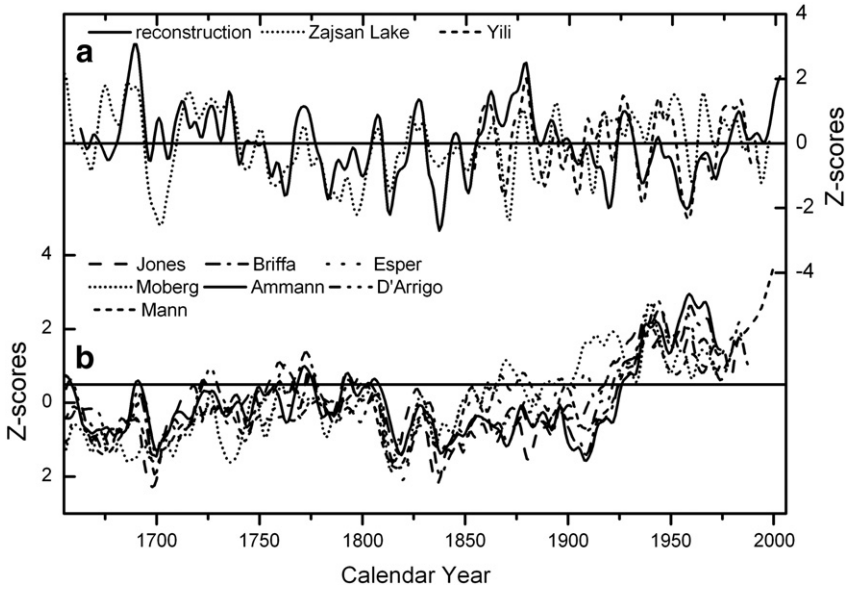

Figure 7. Comparison between the 8-yr low-pass filtered Gongnaisi and: a. summer temperature reconstruction of the Zaysan Lake area (Chen et al., 2011), mean maximum temperature of the Yili (Chen et al., 2009); b. Northern Hemisphere temperature reconstructions (Jones et al., 1998; Briffa et al., 2001; Esper et al., 2002; Moberg et al., 2005; D'Arrigo et al., 2006; Ammann and Wahl, 2007; Mann et al., 2009).

1870 (Fig. 7a). But correlation between our reconstruction and mean maximum temperature for the Yili valley (Chen et al., 2009) was not significant (0.121, $p > 0.05$). The trend of three reconstructions was different after 1880. The reasons of the variation could be caused by human activities of the area. Comparison warm and cold periods, major warm decades (1680s, 1720s–1730s, 1870s) and cold decades (1750s, 1760s, 1780s, 1790s, 1810s) in our reconstruction were also identified in the Zaysan Lake and Yili area (Fig. 7a).

To assess the regional significance of the reconstructed Gongnais May–August minimum temperatures, we calculated spatial correlations between this reconstruction and the CRU gridded dataset (TS3.1) (Mitchell and Jones, 2005) and May–August global sea surface temperatures (SSTs) over the period 1901–2008 using the KNMI Climate Explorer, a web-based collection of climate data analysis tools maintained by the Royal Netherlands Meteorological Institute (http://climexp.knmi.nl). The reconstruction was significantly correlated ($p < 0.05$) with the 8-yr high-pass filtered May–August mean minimum temperatures over large areas of Central Asia (Fig. 8a). The highest correlations with SSTs were concentrated mainly in the equator area of the Indian Ocean and Western Pacific (Fig. 8b). The Indian Ocean was one of the water-vapor sources in the northwest of China. This suggests that the ocean temperature changes can impact on land temperatures of the study area.

We compared our reconstruction to large-scale temperature reconstructions for the Northern Hemisphere (NH) (Jones et al., 1998; Briffa et al., 2001; Esper et al., 2002; Moberg et al., 2005; D'Arrigo et al., 2006; Ammann and Wahl, 2007; Mann et al., 2009). The Gongnaisi series wasn't significantly related to any of the seven Northern Hemisphere temperature reconstructions. As shown in Fig. 7b, there is an increasing trend of our reconstruction value in the recent 30 years, which is of the same phase as global warming. But the increasing trend is not found in temperature reconstructions of the Zaysan and Yili area. Several decadal depressions in the Northern Hemisphere around 1780s, 1810s, 1830s, 1840s and 1970s also occurred in our reconstruction. Although our reconstruction only describes temperature for four months of the year, whereas the Northern Hemisphere temperature reconstructions describe annual temperatures, comparison between the two is justified by the significant annual temperature signals in the GLD used for our reconstruction.

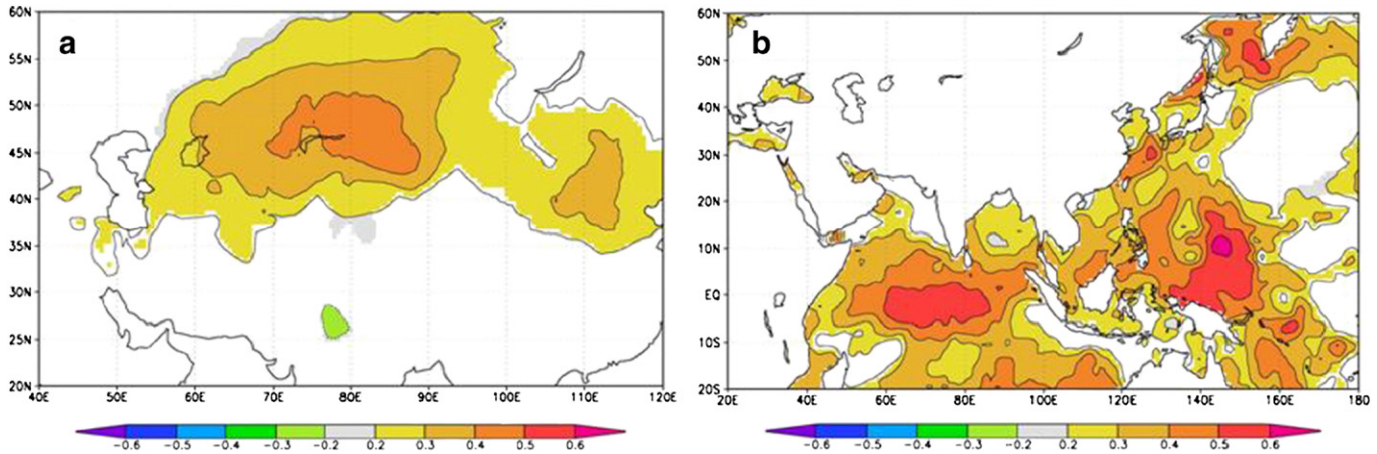

Figure 8. a. Spatial correlations between 8-yr high pass filtered Gongnaisi May–August minimum temperatures and the gridded 0.5° × 0.5°CRU TS 3.1 dataset of monthly surface temperatures; b. Spatial correlations between the temperature reconstruction and the Indo-Pacific SSTs.

https://doi.org/10.1016/j.yqres.2013.05.005 Published online by Cambridge University Press

Conclusions

In this study, a replicated mean latewood density chronology of *P. schrenkiana* was developed and used to infer past May–August minimum temperature variability (AD 1657–2008) for the western Tianshan Mountains. Previous investigations (Polge, 1970; Parker and Henoch, 1971; Briffa et al., 1988; Schweingruber et al., 1988; Briffa et al., 1992; Luckman et al., 1997; Wilson and Luckman, 2003; Büntgen et al., 2005; Büntgen et al., 2008; Wang et al., 2009) found that maximum density and latewood density were significantly associated with climate in their studies.

The temperature reconstruction identified temperature patterns on interannual to centennial time scales, and showed a typically warm May–August from 1657 to 1738, 1855 to 1899 and 1977 to 2008 while the periods 1738–1854 and 1900–1976 were relatively cold. The end of the 20th century is the warmest period in the past 352 yr. Major warm decades (1680s, 1720s–1730s, 1870s) and cold decades (1750s, 1760s, 1780s, 1790s, 1810s) in our reconstruction were also seen in other summer temperature reconstructions from tree-ring records in nearby areas (Chen et al., 2009, 2011). The reconstructed temperature variation appears to have a teleconnection with large-scale atmospheric–oceanic variability and captures long- and broad-scale regional climatic variations.

Acknowledgments

This work was supported by the NSFC project (Nos. 41205070, 41071072, 41275120), Meteorology Public welfare Industry Research Special project (GYHY201206014, GYHY201106013), National Basic Research Program of China (973Program) (No. 2010CB951001), and the Foundation of Xinjiang Laboratory of Tree-ring Ecology (XJYS0911-2009-01).

References

Allan, R., Lindesay, J., Parker, D., 1996. El Niño-Southern Oscillation and Climatic Variability. CSIRO Publishing, Melbourne.
Alward, R.D., Detling, J.K., Milchunas, D.G., 1999. Grassland vegetation changes and nocturnal global warming. Science 283, 229–231.
Ammann, C.M., Wahl, E.R., 2007. The importance of the geophysical context in statistical evaluations of climate reconstruction procedures. Climatic Change 85, 71–88.
Biondi, F., Gershunov, A., Cayan, D.R., 2001. North Pacific decadal climate variability since 1661. Journal of Climate 14, 5–10.
Bräuning, A., Mantwill, B., 2004. Summer temperature and summer monsoon history on the Tibetan Plateau during the last 400 years recorded by tree rings. Geophysical Research Letters 31, L24205. http://dx.doi.org/10.1029/2004GL020793.
Briffa, K.R., Jones, P.D., Schweingruber, F.H., 1988. Summer temperature patterns over Europe: a reconstruction from 1750 AD based on maximum latewood density indices of conifers. Quaternary Research 30, 36–52.
Briffa, K.R., Jones, P.D., Schweingruber, F.H., 1992. Tree-ring density reconstructions of summer temperature patterns across western North America since 1600. Journal of Climate 5, 735–754.
Briffa, K.R., Schweingruber, F.H., Jones, P.D., Osborn, T.J., Shiyatov, S.G., Vaganov, E.A., 1998a. Reduced sensitivity of recent tree-growth to temperature at high northern latitudes. Nature 391, 678–682.
Briffa, K.R., Jones, P.D., Schweingruber, F.H., Osborn, T.J., 1998b. Influence of volcanic eruptions on Northern Hemisphere summer temperature over the past 600 years. Nature 393, 450–455.
Briffa, K.R., Osborn, T.J., Schweingruber, F.H., Harris, I.C., Jones, P.D., Shiyatov, S.G., Vaganov, E.A., 2001. Low frequency temperature variations from a northern tree ring density network. Journal of Geophysical Research 106, 2929–2941.
Büntgen, U., Esper, J., Frank, D.C., Nicolussi, K., Schmidhalter, M., 2005. A 1052-year tree-ring proxy of Alpine summer temperatures. Climate Dynamics 25, 141–153.
Büntgen, U., Frank, D.C., Nievergelt, D., Esper, J., 2006. Summer temperature variations in the European Alps, A.D. 755–2004. Journal of Climate 19, 5606–5623.
Büntgen, U., Frank, D.C., Grudd, H., Esper, J., 2008. Long-term summer temperature variations in the Pyrenees. Climate Dynamics 31, 615–631.
Chang, Z.H., Li, X., 1995. Forest Soil in Mountainous Region of Xinjiang. Xinjiang Science and Technology Press, Urumqi.
Chen, J., Wang, L.L., Zhu, H.F., Wu, P., 2009. Reconstructing mean maximum temperature of growing season from the maximum density of the Schrenk Spruce in Yili, Xinjiang, China. China Science Bulletin 54, 1–9.
Chen, F., Yuan, Y.J., Wei, W.S., Yu, S.L., Li, Y., Zhang, R.B., Zhang, T.W., Shang, H.M., 2010. Chronology development and climate response analysis of Schrenk spruce (*Picea schrenkiana*) tree-ring parameters in the Urumqi river basin, China. Geochrinometria 36, 17–22.
Chen, F., Yuan, Y., Wei, W., Wang, L., Yu, S., Zhang, R., Fan, Z., Shang, H., Zhang, T., Li, Y., 2011. Tree ring density-based summer temperature reconstruction for Zajsan Lake area, East Kazakhstan. International Journal of Climatology 31. http://dx.doi.org/10.1002/joc.2327.
Cook, E.R., 1985. A Time-Series Analysis Approach to Tree-Ring Standardization. (Ph.D. Thesis) Arizona Uni. Press, Tucson.
Cook, E.R., Kairiukstis, L.A., 1990. Methods of Dendrochronology. Kluwer Academic Press, The Netherlands.
D'Arrigo, R.R., Jacoby, G.C., 1999. Northern North American tree-ring evidence for regional temperature change after major volcanic events. Climate Change 41, 1–15.
D'Arrigo, R., Wilson, R.J.S., Jacoby, G.C., 2006. On the long-term context for late 20th century warming. Journal of Geophysical Research 111, D03103. http://dx.doi.org/10.1029/2005JD006352.
D'Arrigo, R., Wilson, R., Liepert, B., Cherubini, P., 2008. On the 'divergence problem' in northern forests: a review of the tree-ring evidence and possible causes. Global and Planetary Change 60, 289–305.
Davi, N., D'Arrigo, R.D., Jacoby, G.C., Buckley, B.M., Kobayashi, O., 2002. Warm-season annual to decadal temperature variability for Hokkaido, Japan, inferred from maximum latewood density (AD 1557–1990) and ring width data (AD 1532–1990). Climate Change 52, 201–217.
Esper, J., 2003. 1300 years of climatic history for Western Central Asia inferred from tree-rings. The Holocene 12, 267–277.
Esper, J., Treydte, K., Gärtner, H., Neuwirth, B., 2001. A tree ring reconstruction of climatic extreme years since 1427 AD for Western Central Asia. Palaeobotanist 50, 141–152.
Esper, J., Cook, E.R., Schweingruber, F.H., 2002. Low-frequency signals in long tree-ring chronologies for reconstructing past temperature variability. Science 295, 2250–2253.
Frank, D., Esper, J., 2005. Temperature reconstructions and comparisons with instrumental data from a tree-ring network for the European Alps. International Journal of Climatology 25, 1437–1454.
Fritts, H.C., 1976. Tree Rings and Climate. Academic Press, London.
Gervais, B.R., MacDonald, G.M., 2001. Tree-ring and summer-temperature response to volcanic aerosol forcing at the northern tree-line, Kola Peninsula, Russia. The Holocene 11, 499–505.
Guiot, J., 1991. The bootstrapped response function. Tree-Ring Buletin 51, 39–41.
Holmes, R.L., 1983. Computer-assisted quality control in tree-ring dating and measurement. Tree-Ring Bulletin 43, 69–75.
Jacoby, G.C., D'Arrigo, R., 1989. Reconstructed Northern Hemisphere annual temperature since 1671 based on high-latitude tree ring data from North America. Climatic Change 14, 39–59.
Jones, P.D., Briffa, K.R., Schweingruber, F.H., 1995. Tree-ring evidence of the widespread effects of explosive volcanic eruptions. Geophysical Research Letters 22, 1333–1336.
Jones, P.D., Briffa, K.R., Barnett, T.P., Tett, S.F.B., 1998. High-resolution palaeoclimatic records for the last millennium: interpretation, integration and comparison with general circulation model control-run temperatures. The Holocene 455–471.
Körner, C., 1998. A re-assessment of high elevation treeline positions and their explanation. Oecologia 115, 445–459.
LaMarch, V.C., Hirschboeck, K.K., 1984. Frost rings in trees as records of major volcanic eruptions. Nature 307, 121–126.
Luckman, B.H., Wilson, R., 2005. Summer temperatures in the Canadian Rockies during the last millennium: a revised record. Climate Dynamics 24, 131–144.
Luckman, B.H., Briffa, K.R., Jones, P.D., Schweingruber, F.H., 1997. Tree ring based reconstruction of summer temperatures at the Columbia Ice field, Alberta, Canada, AD 1073–1983. The Holocene 7, 375–389.
Mann, M.E., Lees, J., 1996. Robust estimation of background noise and signal detection in climatic time series. Climatic Change 33, 409–445.
Mann, M.E., Zhang, Z.H., Rutherford, S., Bradley, R.S., Hughes, M.K., Shindell, D., Ammann, C., Faluvegi, G., Ni, F., 2009. Global Signatures and Dynamical Origins of the Little Ice Age and Medieval Climate Anomaly. Science 326, 1256–1260.
Meehl, G.A., 1987. The annual cycle and interannual variability in the tropical Pacific and Indian Ocean region. Monthly Weather Review 115, 27–50.
Michaelsen, J., 1987. Cross-validation in statistical climate forecast models. Journal of Applied Meteorology and Climatology 26, 1589–1600.
Mitchell, T.D., Jones, P.D., 2005. An improved method of constructing a database of monthly climate observations and associated high resolution grids. International Journal of Climatology 25, 693–712.
Moberg, A., Sonechkin, D.M., Holmgren, K., Datsenko, N.M., Karlén, W., 2005. Highly variable Northern Hemisphere temperatures reconstructed from low-and high-resolution proxy data. Nature 433, 613–617.
Parker, M.L., Henoch, W.E.S., 1971. The use of Engelmann spruce latewood density for dendrochronological purposes. Canadian Journal of Forest Research 1, 90–98.
Peterson, D.W., Peterson, D.L., 2001. Mountain hemlock growth responds to climatic variability at annual and decadal time scales. Ecology 82, 3330–3345.
Polge, H., 1970. The use of X-ray densitometric methods in dendrochronology. Tree-Ring Bulletin 30, 1–10.
Rayner, N.A., Parker, D.E., Horton, E.B., Folland, C.K., Alexander, L.V., Rowell, D.P., Kent, E.C., Kaplan, A., 2003. Global analyses of sea surface temperature, sea ice, and night marine air temperature since the late nineteenth century J. Journal of Geophysical Research 108 (D14), 4407. http://dx.doi.org/10.1029/2002JD002670.

Schweingruber, F.H., Briffa, K.R., 1996. Tree-ring density networks of climate reconstruction. In: Jones, P.D., Bradley, R.S., Jouzel, J. (Eds.), Climatic Variations and Forcing Mechanisms of the Last 2000 Years: NATO ASI Series, 41, pp. 43–66.

Schweingruber, F.H., Bartholin, T., Schär, E., Briffa, K.R., 1988. Radiodensitometric-dendroclimatological conifer chronologies from Lapland (Scandinavia) and the Alps (Switzerland). Boreas 17, 559–566.

Schweingruber, F.H., Briffa, K.R., Nogler, P., 1993. A tree-ring densitometric transect from Alaska to Labrador: comparison of ring-width and maximum-latewood-density chronologies in the conifer belt of northern North America. International Journal of Biometeorology 37, 151–169.

Simkin, T., Siebert, L., 1994. Volcanoes of the World: A Regional Directory, Gazetteer, and Chronology of Volcanism during the Last 10,000 Years. Geoscience Press, Tucson.

Wang, L.L., Duan, J.P., Chen, J., Huang, L., Shao, X.M., 2009. Temperature reconstruction from tree-ring maximum density of Balfour spruce in eastern Tibet, China. International Journal of Climatology 30, 972–979.

Wigley, T.M.L., Briffa, K.R., Jones, P.D., 1984. On the average value of correlated time series, with applications in dendroclimatology and hydrometeorology. Journal of Climate and Applied Meteorology 23, 201–213.

Wilson, R., Luckman, B.H., 2003. Dendroclimatic reconstruction of maximum summer temperatures from upper treeline sites in Interior British Columbia, Canada. The Holocene 13, 851–861.

Yuan, Y.J., Li, J.F., 1999. Reconstruction and analysis of 450 years winter temperature series in the Urumqi River source of Tianshan Mountains. Journal of Glaciology and Geocryology 21, 64–70.

Yuan, Y.J., Li, J.F., Zhang, J.B., 2001. 348-year precipitation reconstruction from tree-rings for the north slope of the middle Tianshan Mountains. Acta Meteorologica Sinica 15, 95–104.

Yuan, Y.J., Jin, L.Y., Shao, X.M., He, Q., Li, Z.Z., Li, J.F., 2003. Variations of the spring precipitation day numbers reconstructed from tree rings in the Urumqi River drainage, Tianshan Mts. over the last 370 years. Chinese Science Bulletin 48, 1507–1510.

https://doi.org/10.1016/j.yqres.2013.05.005 Published online by Cambridge University Press